Current Research in Food Science 7 (2023) 100589

Contents lists available at ScienceDirect

Current Research in Food Science

journal homepage: www.sciencedirect.com/journal/current-research-in-food-science

A novel method for obtaining high amylose starch fractions from debranched starch

Zhongchao He, Chengdeng Chi, Shuangxia Huang, Xiaoxi Li *

Ministry of Education Engineering Research Center of Starch and Protein Processing, Guangdong Province Key Laboratory for Green Processing of Natural Products and Product Safety, School of Food Science and Engineering, South China University of Technology, Guangzhou, 510640, China

ARTICLE INFO

Handling Editor: Professor Aiqian Ye

Keywords:
Amylose
Short-term retrogradation
Debranched starch
Chain length distribution
Retrogradation behavior

ABSTRACT

High amylose starch shows wide applications in food and non-food-based industries. Traditional complex-precipitation approach for the amylose fractionation required a large volume of organic reagents and was possibly risky for food safety. The object of this work was to establish a novel method to obtain starch fractions rich in amylose from debranch starch through repeated short-term retrogradation and centrifugation. Four starch fractions were obtained with the amylose content of 52.08% (C1), 62.28% (C2), 63.58% (C3), and 64.74% (C4). The thermograms of samples displayed that multiple endothermic peaks were detected in C1 and C2 and only one endothermic peak with melting temperature over 120 °C were observed in C3 and C4, indicating their differences in retrogradation behavior. The chain length distribution results of sample exhibited that C1 and C2 contained more short chains (DP $\leq$ 24), while C3 and C4 consisted of mainly long chains (DP $\geq$ 25). Accordingly, the differences in fine structures could provide more choices for these fractionated high amylose starch to utilize in practical applications.

1. Introduction

Starch, a highly abundant biomass in the world, consists of two groups of glucose polymers: amylose (AM) and amylopectin (AP). The former which accounts for about 20–30% is a linear AM, including largely AM and some linear segments with side chains, while the latter which has a proportion of 70–80% is forked AP branched by alpha-1,6 glycosidic bonds on the basis of AM, including two major groups of short (S) and long (L) chains divided by being at degree of polymerization (DP) ~36 (Bertoft, 2017; Lovegrove et al., 2017). S and L chains are further sub-divided into A chains (with average DP 6–12), B_1 chains (DP 13–24), B_2 chains (DP 25–36) and B_{3+} chains (DP $\geq$ 37) by Hanashiro et al. (1996). Recently, AM has attracted a great deal of attention due to its special structures and functions. It not only owns an excellent nanohelical structure which has advantages in encapsulating and carrying guest molecules (fatty acids, antioxidants, flavors, emulsifiers and surfactants) (Gelders et al., 2006; Kong et al., 2018; Zhu, 2017), but also has properties and functions differed from native starch, including viscoelasticity, gelatinization, crystallization and digestibility (Rodriguez-Garcia et al., 2021; Wani et al., 2012). For example, AM contributes to improving the stability and increasing the viscosity of milk beverages (Lu et al., 2019), which represented food products with high quality and well texture. Numerous studies have also found that the high resistance to enzymes of AM can improve satiety and reduce blood sugar level (Zhu et al., 2022).

Currently, there are three main approaches can be utilized for obtaining AM: enzymatic synthesis, leaching of native starch, complex-precipitation (Doblado-Maldonado et al., 2017). α-D-glucose-1-phosphate was usually used during synthesizing which can provide AM fractions with low polydispersity and the controlled average degree of polymerization (DP) via manipulating the reaction condition. The second is based on the fact that AM can be leached from starch granule during heating above the gelatinization temperature. Due to AP can also be introduced, the low purity of AM is still a burning problem needed to be settled. For this purpose, anneal and ultracentrifugation have been considered as selectable ways to purify AM extracts. Compared with the above methods, complex-precipitation is more common and effective, AM derived from debranched starch is required to completely disperse in the solution for complexation with precipitants (often organic solvents), causing apparent differences in solubility between the resultant complex and AP. However, the most crucial step is to efficiently remove the precipitants from AM complexes. The result is rather polydisperse

* Corresponding author.
E-mail address: xxlee@scut.edu.cn (X. Li).

https://doi.org/10.1016/j.crfs.2023.100589
Received 19 May 2023; Received in revised form 4 August 2023; Accepted 7 September 2023
Available online 9 September 2023

AM with large molar mass and high purity can be collected. Although this method of isolating AM is widely used, it needs to consume a large volume of organic solvents and take inevitable tedious steps, such as dispersion and evaporation. Hence, it is important to explore new precipitants for AM extraction.

It is notable that short-term retrogradation is a special feature for AM, starch chains are neatly aligned by hydrogen bonds to form semi-crystalline or crystalline within a few hours, which can lead to density differences with AP. At this point, AM can be allowed as a self-precipitant and obtained through centrifugation with suitable centrifugal force. So, the purpose of the present work was to investigate the potential of AM as a precipitant and obtain starch fractions rich in AM from debranched starch using a novel method. Additionally, molecular weight distribution, degree of branching, and chain length distribution of starch extracts were determined in order to provide helpful information for the development and application of AM.

2. Materials and methods

2.1. Materials

Potato starch (PS) was supplied by Pengyuan starch Co., Ltd. (Qinghuangdao, China). Pullulanase (1000 U/g) was supplied by Yuanye Bio-Technology Co., Ltd (Shanghai, China). Iodine and potassium iodide were obtained from Macklin (Shanghai, China).

2.2. Removal of lipids

The method described by Ye et al. (2018), with some minor modifications, were used to remove lipids from potato starch. PS (600 g, dry basis) was blended with 1500 mL petroleum ether and continuously stirring at room temperature for 5 h. Filtration was carried out, and the solid residues were obtained. Finally, PS without lipids was dried and stored in hermetically sealed glass bottles.

2.3. Starch separation and purification

Starch was firstly debranched as follows and the sample mixed with AM and AP was obtained. PS without lipids (180 g, dry basis) was homogeneously dispersed in 1800 mL of deionized water and cooked in boiling water for completely gelatinization. The gelatinized starch was cooled to 55 °C and adjusted to pH 5.0, and pullulanase (150 U/g of dry starch) was added. The mixture was incubated at 55 °C for 12 h. The mixture was later adjusted to pH 7.0 and heated at 100 °C for 30 min to inactivate the pullulanase. Finally, the product named DPS was collected.

AM was purified through repeated cooling and centrifugation treatments. DPS was suspended in deionized water (500 mL) with continuous stirring and stood at 25 °C for 30 min. The starch solution was then centrifuged at 4390×*g* for 10 min and then the precipitate obtained through first centrifugation was named C1. According to our previous investigation, it was found that cooking before storage could facilitate short-term retrogradation. Hence, C1 was dissolved in deionized water (500 mL) and cooked at 100 °C for 30 min, following by centrifugation. Afterwards, the above procedure except centrifugal force was repeated to obtain other fractions. These samples were named as C2, C3, and C4, which denoted the precipitates collected from the second (2809×*g*), third (1580×*g*), fourth (702×*g*) centrifugation, respectively. The detailed procedure for separation and purification of AM is shown in Fig. 1. Each fraction was washed with three times of distilled water as well as ethanol before freeze-dried. The dried starch fractions were weighed to evaluate the yields of each procedure.

2.4. Assay for AM content

The apparent amylose content (AC) of starch samples was determined by using the iodine reagent method (Tan et al., 2017). 100 mg of starch was accurately weighed and dispersed in a 1 M NaOH solution (9 mL), which was then diluted with distilled water to obtain a 1 mg/mL solution. Mixed 2.5 mL of the diluted solution with 25 mL of deionized water, then added with 1 mL of 1 M acetic acid solution and 1 mL of 0.2% iodine solution, and made up to 50 mL with distilled water. This solution was measured at 620 nm using an UV–Visible Spectrophotometer (Thermo Scientific, USA). AC value was determined using a standard curve established by a mixed solution of amylose (A0512, Sigma-Aldrich) and amylopectin (A8515, Sigma-Aldrich).

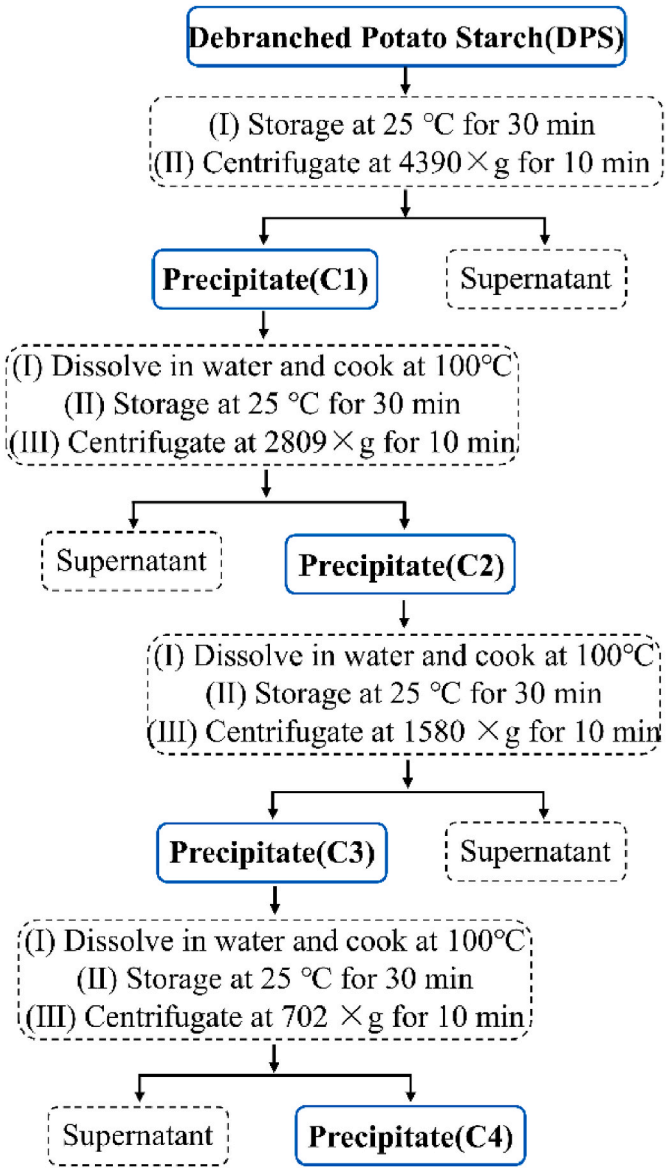

Fig. 1. Illustration of procedure for purification of starch fractions.

2.5. Gel permeation chromatography coupled with multi-angle light scattering and a refractive index detector (GPC-MALS-RI)

The weight-average molecular weight (M_w) of starch samples was collected through a GPC (Waters, USA) equipped with a MALS detector and a differential refractive index detector (Wyatt Technology Co., USA) and analyzed through Astra V software program (Tu et al., 2021). Around 5 mg of sample was completely dissolved in 5 mL of degassed DMSO solution (mobile phase) containing LiBr (50 mmol/L) and filtered through a 5 μm PTFE filter film (Millipore Co., USA). All samples were

injected into the GPC system equipped with OHpak SB-806HQ and SB-804HQ columns (Showdex Denko, Japan) and analyzed under 40 °C of the column temperature, 658 nm of the detected wavelength and 0.3 mL/min of the flow rate.

2.6. Differential scanning calorimeter (DSC)

Thermal properties of starch fractions were measured using a DSC (PerkinElmer, USA) and calculated based on the dry starch basis by using Pyris software (PerkinElmer) (Huang et al., 2022). Each sample (approximately 5 mg) was suspended with double amount of water and equilibrated at 25 °C for 24 h. Then the sample was placed in an aluminum pan and the container was hermetically sealed by gold foil. The pans were heated from 20 to 150 °C at a heating rate of 10 °C/min in a nitrogen atmosphere during testing.

2.7. ^1H Nuclear magnetic resonance (NMR)

All samples were dried at 60 °C for 1 h, then transferred to NMR tubes and dissolved in DMSO-d_6. The dissolved samples were measured on a Bruker Avance 600 spectrometer (Bruker, Germany) operating at 500 MHz at 30 °C with a relaxation delay of 10 s and 128 scans. Degrees of branching were determined from Nilsson et al. (1996).

2.8. High-performance anion exchange chromatography coupled with pulsed amperometric detection

Chain length distribution of the samples was analyzed by using a high-performance anion-exchange chromatograph system with pulsed amperometric detection (Thermo Fisher, USA.). Samples of starch (10 mg) were dissolved in 90% DMSO (450 μL) and double distilled water (2250 μL), sodium acetate buffer (300 μL, pH 4.5), solution of NaN3 (5 μL) and isoamylase (5 μL) were added. The diluted solution was then stand at 38 °C for 24 h. Afterwards, the supernatant obtained from the hydrolysate through centrifuging at 12000 rpm for 5 min was injected into the Thermo ICS-5000+ system with the DionexTM CarboPacTM PA10 (4 mm × 250 mm, 10 μm) column at 30 °C to determine average chain length. The flow rate was 0.3 mL/min and the injection volume was 20 μL. The mobile phases were eluent A (0.2 M NaOH) and eluent B (0.2 M NaOH containing 0.2 M sodium acetate). A gradient elution was used as follows: 0–14 min, 10% B; 14–17.1 min, 60% B; 17.1–22min, 10% B.

2.9. Statistical analysis

All tests were conducted at least in triple and the data were statistically analyzed for differences using LSD and Duncan's Multiple Range Test at a level of 0.05 with SPSS (USA).

3. Results and discussion

3.1. Yields of starch fractions

The yields of starch fractions under each procedure were shown in Figure. A1. The yields of C1, C2, C3 and C4 were 75.02%, 61.28%. 79.29% and 87.41%, respectively. This mainly ascribed to the differences in short-term retrogradation behaviours of starch molecules of starch fractions, which led to a different fate during centrifugation, and in turn affected the yields of starch fractions.

3.2. Short-term retrogradation behaviors of starch fractions

Thermoanalysis was proved to be an effective approach to quantify the crystallinity of AM crystallite. Specially the phase transition of the crystallite occurring at a higher temperature was detected and easily differentiated from that of AP (Tian et al., 2009). The thermal thermogram and parameters of starch fractions are shown in Fig. 2 and Table 1. It was observed that there were two broad endothermic peaks in DPS appearing at approximately 79 °C and 125 °C, which were attribute to the melting of hybrid starch crystals packed with AP and AM. Moreover, the former was mainly composed of AP, while the latter consisted mainly of AM, despite the low melting enthalpy changes (ΔH). Liu et al. (2006) reported that a maximum of four endotherms were detected in a mixture of AM and AP with about 50% water content and they were assigned to the gelatinization of AP (about 70 °C), non-equilibrium melting of crystallites (a shoulder overlapped with AP), the phase transition of amylose–lipid complex (about 100 °C), and the melting of AM crystals (over 100 °C) according to the temperature of endothermic peaks. The detected peaks in DPS may be due to partially retrogradation of starch molecules during water equilibration before DSC test, and they were not observed in C1 at the same temperature after short-term retrogradation and centrifugation. Actually, C1 exhibited three relatively narrow endothermic peaks in the thermogram at about 90 °C, 100 °C and 115 °C, whose corresponding ΔH were 3.41, 5.74 and 10.08 J/g, respectively. This could be attributed to the differentially rearrangement of AM with different chain lengths during short-term retrogradation. Similarly, Boonna and Tongta (2018) also reported that two similar endothermic peaks appeared during DSC analysis of debranched starch, which were caused by the melting of intermediate and longer linear glucans and the dissociation of recrystallized native AM, respectively. Accordingly, these results indicated that AM could rearrange during 30 min of storage to form starch ordered structures and be obtained through centrifugation.

With further purification, it was observed that there were two endothermic peaks in C2 occurring at about 90 °C with ΔH of 11.75 J/g and 120 °C with ΔH of 14.06 J/g, respectively, which indicated the increased ordered structures. Starch retrogradation involved three phases of crystallization observed as three sequential steps: nucleation, growth of crystals, and maturation. Generally, the existing crystalline nuclei or crystal seeds could promote the aggregation of AM and increase the content of ordered structures (Zhu et al., 2020). Before short-term retrogradation, the ordered structures matched Peak I of C1 were completely destroyed and the ordered structures matched Peak II of C1 partial melted during cooking at 100 °C. Contrarily, the ordered structures matched with Peak III was well-preserved after cooking. Hence, the ordered structures matched with Peak II and III of C1 may act as crystal seeds and involve in the rearrangement of AM. The starch chains that remained in C1 after centrifugation thereby aggregated towards the above crystal seeds and arranged in an ordered manner enabling the crystal grain to grow. The growth of crystals with

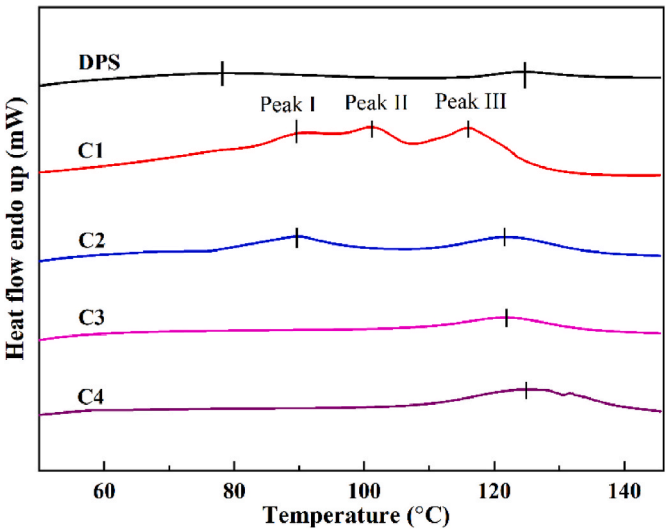

Fig. 2. DSC curve of starch fractions.

Table 1
The onset, peak, and conclusion temperature (T_o, T_p, and T_e) and enthalpy change (ΔH) of starch fractions. Values are given as mean (n = 3). Different letters in the same column indicate significantly different ($p < 0.05$).

Sample	Peak I				Peak II				Peak III			
	T_o (°C)	T_p (°C)	T_e (°C)	ΔH (J/g)	T_o (°C)	T_p (°C)	T_e (°C)	ΔH(J/g)	T_o (°C)	T_p (°C)	T_e (°C)	ΔH (J/g)
DPS	62.33^{c}	78.99^{b}	101.16^{a}	8.35^{b}	–	–	–	–	116.24^{a}	124.65^{a}	134.51^{c}	4.89^{e}
C1	84.46^{a}	91.24^{a}	94.90^{c}	3.41^{c}	96.79^{a}	101.39^{a}	106.04^{a}	5.74^{a}	109.78^{b}	116.57^{c}	129.28^{d}	10.08^{d}
C2	76.42^{b}	89.66^{a}	98.54^{b}	11.75^{a}	–	–	–	–	110.87^{b}	121.65^{b}	135.38^{b}	14.06^{c}
C3	–	–	–	–	–	–	–	–	107.90^{c}	121.66^{b}	134.65^{bc}	18.22^{b}
C4	–	–	–	–	–	–	–	–	108.68^{c}	124.70^{a}	139.83^{a}	26.99^{a}

heterogeneity caused that one broad endothermic peak with a phase transition temperature range ($T_c - T_o$) of 22.12 °C and one with a phase transition temperature range ($T_c - T_o$) of 24.51 °C were detected at a low and high temperature, respectively. Notably, C3 and C4 both displayed only one broad endothermic peak with a phase transition temperature range ($T_c - T_o$) of 26.75 °C and 31.15 °C, respectively. This indicated that the formation of AM crystallites with greater heterogeneity (Villas-Boas et al., 2020). Moreover, the latter showed the higher ΔH and peak temperature (T_p) compared to the former, which suggested that C4 contained more and stronger ordered structures composed of AM.

3.3. Apparent amylose content (AC) and debranching degree (DB)of starch fractions

Iodine-based colorimetry was used to determine AC value and DB of starch fractions was analyzed by ^{1}H NMR spectrum. The results were put in Table 2. AC and DB value of samples increased from 30.06% to 42.70% and decreased from 8.09% to 7.74%, respectively. This indicated that enzymatic hydrolysis of side chains of AP by pullulanase. After short-term retrogradation and centrifugation, AC value of starch sample further increased to 52.08% of C1 with accompanying DB value of 7.02%. This phenomenon might be explained as follows. Amorphous AM aggregated and then interacted with each other through hydrogen bonds to form starch ordered structures and was collected via centrifugation, which also reflected by the endothermic peaks in DSC. While, AP was not inclined to rearrange and involve in short-term retrogradation, causing these AP with suitable molecular weight were removed through centrifugation at 4390×*g*. With repeated short-term retrogradation, AC value of samples showed a growing trend, implying an increasing AM were subjected to the formation of starch ordered structures. Meanwhile, as repeated centrifugation with decreasing centrifugal force, DB value of samples exhibited a declining trend, suggesting an increasing AP was centrifuged to the supernatant. The results of AC and DB value indicated that the combination of ordered structures formed by short-term retrogradation and continuous removal of AP through centrifuging with decreasing centrifugal force may cause the increased purity of AM in starch fractions.

3.4. Changes in distribution of weight-average molecular weight

The GPC-RI chromatogram of starch fractions are shown in Fig. 3. For native potato starch (PS), there were two elution peaks in the RI profile. The first major peak (Peak 1) corresponded to AP and/or long

Table 2
Amylose content (AC) and branching degree (DB) of starch fractions. Values are given as mean (n = 3). Different letters in the same line indicate significantly different ($p < 0.05$).

Sample	PS	DPS	C1	C2	C3	C4
AC (%)	30.06 ± 0.54^{f}	42.70 ± 0.66^{e}	52.08 ± 0.21^{d}	62.28 ± 0.19^{c}	63.58 ± 0.42^{b}	64.74 ± 0.37^{a}
DB (%)	8.09 ± 0.11^{a}	7.74 ± 0.15^{b}	7.02 ± 0.13^{c}	4.83 ± 0.17^{d}	4.39 ± 0.15^{e}	4.29 ± 0.12^{e}

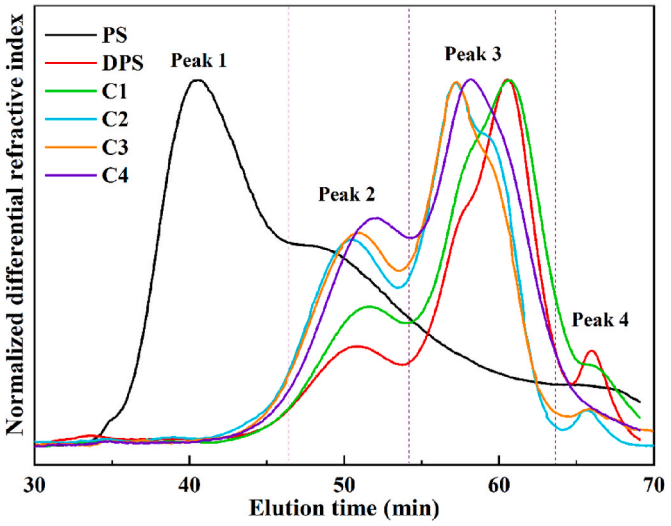

Fig. 3. GPC-RI chromatogram of starch fractions.

AM chains, followed by the second peak (Peak 2) denoted AM and the long side chains of AP. Notably, it was observed that the tailing appeared after 54 min, which may be attribute to the short side chains of AP (Radosta et al., 2016). After pullulanase treatment, DPS exhibited three clear elution peaks after Peak 1, indicating the degradation of PS. In contrast to the profile of native starch, two extra peaks (Peak 3 and Peak 4) were mainly assigned to AM derived from degraded side chains with different molecular weights. With repeated retrogradation, the peak intensity of Peak 4 gradually decreased, while Peak 2 showed an increasing intensity. This indicated that these starch fractions were continuously collected through repeated retrogradation and centrifugation. On the contrary, AM with short chains does not trend to rearrange during storage (Cai and Shi, 2010), causing these starch chains were dispersed in the solution and removed after centrifugation.

The GPC-MALLS profile of starch fractions was shown in Figure. A2 and the molecular weight distribution of starch fractions was placed in Table 3. The degradation of pullulanase reduced the M_w of PS by 2 orders of magnitude. After DPS was cooled and centrifuged, the proportion of starch with M_w smaller than 5000 g/mol in C1 decreased, corresponding to the reduction of starch chains with low molar mass. Notably, when C1 was heating before purification, C2 exhibited the decreased fractions of <5000 g/mol and 5000–10000 g/mol and the increased fractions of 10000-50000 g/mol and 50000-90000 g/mol. Chi et al. (2023) reported that starch ordered structures packed with long AM had higher thermostability compared to short AM. As described in 3.1, diverse retrogradation behaviors of starch chains induced the formation of ordered structures with different thermal stability in C1 and further exerted an impact on subsequent retrogradation after heating. As purification with a drop of the centrifugal force gradually, the proportion of starch fragments with $M_w < 5000$ g/mol and $10000 < M_w < 50000$ g/mol increased. It can be speculated that the starch ordered structures were mainly composed of fragments with $M_w < 5000$ g/mol

Table 3
Weight-average molecular weight and its distribution of starch fractions. Deviation of results are in brackets.

Samples	M_w (g/mol)	Molar mass distribution (%)				
		<5000 g/mol	5000–10000 g/mol	10000-50000 g/mol	50000-90000 g/mol	>90000 g/mol
PS	7.85×10^6 (1%)	–	–	–	–	100
DPS	4.85×10^4 (4%)	53.15	9.04	17.07	11.27	9.47
C1	8.50×10^4 (3%)	38.73	13.39	22.42	14.14	11.32
C2	6.22×10^4 (3%)	36.92	10.05	26.29	17.25	9.49
C3	5.47×10^4 (4%)	37.07	8.57	27.42	16.85	10.09
C4	4.95×10^4 (2%)	38.40	7.73	32.52	9.04	12.31

and $10000 < M_w < 50000$ g/mol. Additionally, the percentage of starch fragments with $5000 < M_w < 10000$ g/mol and $50000 < M_w < 90000$ g/mol declined, indicating these starch fragments mainly were removed by centrifuging.

3.5. Chain length distribution (CLD) of debranched starch

The CLD results of different starch fractions derived from debranched starch were shown in Table 4. After debranching with pullulanase, DPS consisted of mainly B_1 chains, in line with the CLD results of native potato starch reported by Jung et al. (2022). In term of A chains, the amount of them decreased from 19.41% of DPS to 7.33% of C4. According to Cai and Shi (2010), these starch chains with short length, especially DP < 10, were below the minimum chain length allowed to form starch double helices and thus remained in the solution. B_1 chains with medium length (DP 13–24) preferred to form helical structures and acted as the main component of starch fractions, although the content of them deceased with repeated purifications. As for B_2 and B_{3+} chains, the amount of these long chains (DP ≥ 25) differed from A and B_1 chains exhibited an increased trend during purification. Chang et al. (2019) revealed that the chain length of debranched starch chains was positively correlated with the rate of retrogradation. Nevertheless, short chains (DP ≤ 24) dominated the chain length distribution in isolated fractions over the first two retrogradation, while starch fractions contained more long chains under subsequent retrogradation. This indicated that long chains aggregated and rearranged inferior to short chains within short time and dispersed in the solution similar to AP, whereas were not removed during centrifugation.

Table 4
Chain length distribution (CLD) of starch fractions. Data are expressed as the mean ± standard deviation (n = 3). Different letters in the same column indicate significantly different ($p < 0.05$).

Samples	Average DP	CLD (%)			
		A (DP 6–12)	B_1 (DP 13–24)	B_2 (DP 25–36)	B_{3+} (DP ≥ 37)
DPS	22.72 ± 0.01^e	19.41 ± 0.43^a	49.87 ± 0.19^a	15.02 ± 0.11^e	15.72 ± 0.12^e
C1	24.94 ± 0.24^d	14.98 ± 0.25^b	47.27 ± 0.81^b	17.33 ± 0.38^d	20.43 ± 0.67^d
C2	28.17 ± 0.20^c	10.60 ± 0.01^c	41.97 ± 0.04^c	19.34 ± 0.37^c	28.10 ± 0.42^c
C3	29.62 ± 0.24^b	8.93 ± 0.11^d	39.01 ± 0.01^d	20.50 ± 0.42^b	31.58 ± 0.53^b
C4	30.81 ± 0.34^a	7.33 ± 0.10^e	36.95 ± 0.22^e	21.25 ± 0.36^a	34.50 ± 0.70^a

3.6. Underlying mechanism for the fractionation of high amylose starch fractions

The mechanism representation for obtaining high amylose starch fractions and the changes in fine structures of starch fractions during purifying AM were shown in Fig. 4. After gelatinization at high temperature and enzymatic hydrolysis by pullulanase, most of the alpha-1,6 glycosidic bonds of native potato starch molecules were broken, resulting in a large number of AM with different chain length (Table 2, Table 4), and a small amount of AP with different molar mass (Table 2, Table 3). During short-term retrogradation, these starch molecules formed different ordered structures with melting temperature of 91.24 °C, 101.39 °C and 116.57 °C (Table 1) and were collected through centrifugation. When cooking was involved before storage, the ordered structures with low melting temperature were destroyed during heating, whereas the ordered structures with high melting temperature were remained and acted as crystal seeds to facilitated the rearrangement of AM during subsequent retrogradation (Zhu et al., 2020). With repeated retrogradation and centrifugation, more AM with long chain length and high molar mass started to retrogradation (Table 3, Table 4), causing that short chains replaced long chains as the dominant constituent for starch fractions. While, as centrifugation with a decreasing centrifugal force, more AP was continuously removed according to molar mass (Table 2, Table 3). Therefore, starch fractions with higher AM ratio and lower AP ratio could be obtain through short-term retrogradation and centrifugation.

4. Conclusion and perspectives

In summary, we proved that AM could serve as a self-precipitant and thus the content of AM in starch fraction significantly increased through short-term retrogradation and centrifugation. Hence, a novel method was proposed and established to prepare starch fractions rich in AM. Four starch fractions with AC content of 52.08%–64.74% were finally obtained according to the difference in retrogradation behavior of different starch molecules. The M_w of all starch samples were 8.50×10^4, 6.22×10^4, 5.47×10^4, and 4.95×10^4 g/mol, respectively. CLD analysis revealed that C1 and C2 contained more short AM chains (DP ≤ 24), while C3 and C4 were dominated by long AM chains (DP ≥ 25). Although this work verified that short-term retrogradation could be used for fractionating starch fractions rich in AM, how temperature, time and water content during storage affected the fractionation efficiency of AM should be further investigated in the future. Furthermore, the differences in physicochemical properties and functions of starch fractions caused by resultant fine structures were also in our future works for better application in the food industry.

CRediT authorship contribution statement

Zhongchao He: Data curation, Writing – original draft. **Chengdeng Chi:** Formal analysis, Methodology, Investigation. **Shuangxia Huang:** Formal analysis, Visualization, Validation. **Xiaoxi Li:** Project administration, Writing – review & editing.

Declaration of competing interest

The authors declare that they have no known competing financial interests or personal relationships that could have appeared to influence the work reported in this paper.

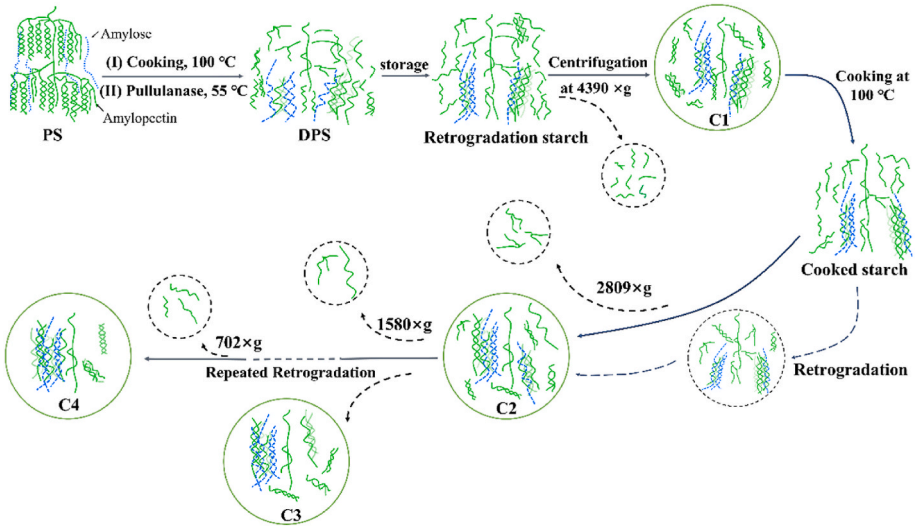

Fig. 4. The structural changes of starch molecules in the process of purification.

Data availability

Data will be made available on request.

Acknowledgements

This work is supported by the National Natural Science Foundation of China (32072172, 32172238).

Appendix A. Supplementary data

Supplementary data to this article can be found online at https://doi.org/10.1016/j.crfs.2023.100589.

References

Bertoft, E., 2017. Understanding starch structure: recent progress. Agronomy 7 (3), 56. https://doi.org/10.3390/agronomy7030056.

Boonna, S., Tongta, S., 2018. Structural transformation of crystallized debranched cassava starch during dual hydrothermal treatment in relation to enzyme digestibility. Carbohydr. Polym. 191, 1–7. https://doi.org/10.1016/j.carbpol.2018.03.006.

Cai, L., Shi, Y.C., 2010. Structure and digestibility of crystalline short-chain amylose from debranched waxy wheat, waxy maize, and waxy potato starches. Carbohydr. Polym. 79 (4), 1117–1123. https://doi.org/10.1016/j.carbpol.2009.10.057.

Chang, R., Li, M., Wang, Y., Chen, H., Xiao, J., Xiong, L., Qiu, L., Bian, X., Sun, C., Sun, Q., 2019. Retrogradation behavior of debranched starch with different degrees of polymerization. Food Chem. 297, 125001 https://doi.org/10.1016/j.foodchem.2019.125001.

Chi, C., Zhou, Y., Chen, B., He, Y., Zhao, Y., 2023. A facile method for classifying starch fractions rich in long linear dextrin. Food Hydrocolloids 135, 108182. https://doi.org/10.1016/j.foodhyd.2022.108182.

Doblado-Maldonado, A.F., Gomand, S.V., Goderis, B., Delcour, J.A., 2017. Methodologies for producing amylose: a review. Crit. Rev. Food Sci. Nutr. 57 (2), 407–417. https://doi.org/10.1080/10408398.2014.954030.

Gelders, G.G., Goesaert, H., Delcour, J.A., 2006. Amylose−Lipid complexes as controlled lipid release agents during starch gelatinization and pasting. J. Agric. Food Chem. 54 (4), 1493–1499. https://doi.org/10.1021/jf051743c.

Hanashiro, I., Abe, J., Hizukuri, S., 1996. A periodic distribution of the chain length of amylopectin as revealed by high-performance anion-exchange chromatography. Carbohydr. Res. 283, 151–159. https://doi.org/10.1016/0008-6215(95)00408-4.

Huang, S., Chi, C., Li, X., Zhang, Y., Chen, L., 2022. Understanding the structure, digestibility, texture and flavor attributes of rice noodles complexation with xanthan and dodecyl gallate. Food Hydrocolloids 127, 107538. https://doi.org/10.1016/j.foodhyd.2022.107538.

Jung, D.H., Park, C.S., Kim, H.S., Nam, T.G., Lee, B.H., Baik, M.Y., Yoo, S.H., Seo, D.H., 2022. Enzymatic modification of potato starch by amylosucrase according to reaction temperature: effect of branch-chain length on structural, physicochemical, and digestive properties. Food Hydrocolloids 122, 107086. https://doi.org/10.1016/j.foodhyd.2021.107086.

Kong, L., Bhosale, R., Ziegler, G.R., 2018. Encapsulation and stabilization of β-carotene by amylose inclusion complexes. Food Res. Int. 105, 446–452. https://doi.org/10.1016/j.foodres.2017.11.058.

Liu, H., Yu, L., Xie, F., Chen, L., 2006. Gelatinization of cornstarch with different amylose/amylopectin content. Carbohydr. Polym. 65 (3), 357–363. https://doi.org/10.1016/j.carbpol.2006.01.026.

Lovegrove, A., Edwards, C.H., De Noni, I., Patel, H., El, S.N., Grassby, T., Shewry, P.R., 2017. Role of polysaccharides in food, digestion, and health. Crit. Rev. Food Sci. Nutr. 57 (2), 237–253. https://doi.org/10.1080/10408398.2014.939263.

Lu, X., Su, H., Guo, J., Tu, J., Lei, Y., Zeng, S., Chen, Y., Miao, S., Zheng, B., 2019. Rheological properties and structural features of coconut milk emulsions stabilized with maize kernels and starch. Food Hydrocolloids 96, 385–395. https://doi.org/10.1016/j.foodhyd.2019.05.027.

Nilsson, G.S., Gorton, L., Bergquist, K.E., Nilsson, U., 1996. Determination of the degree of branching in normal and amylopectin type potato starch with 1H-NMR spectroscopy improved resolution and two-dimensional spectroscopy. Starch Staerke 48 (10), 352–357. https://doi.org/10.1002/star.19960481003.

Radosta, S., Kiessler, B., Vorwerg, W., Brenner, T., 2016. Molecular composition of surface sizing starch prepared using oxidation, enzymatic hydrolysis and ultrasonic treatment methods. Starch Staerke 68 (5–6), 541–548. https://doi.org/10.1002/star.201500314.

Rodriguez-Garcia, M.E., Hernandez-Landaverde, M.A., Delgado, J.M., Ramirez-Gutierrez, C.F., Ramirez-Cardona, M., Millan-Malo, B.M., Londoño-Restrepo, S.M., 2021. Crystalline structures of the main components of starch. Curr. Opin. Food Sci. 37, 107–111. https://doi.org/10.1016/j.cofs.2020.10.002.

Tan, X., Gu, B., Li, X., Xie, C., Chen, L., Zhang, B., 2017. Effect of growth period on the multi-scale structure and physicochemical properties of cassava starch. Int. J. Biol. Macromol. 101, 9–15. https://doi.org/10.1016/j.ijbiomac.2017.03.031.

Tian, Y., Li, Y., Jin, Z., Xu, X., 2009. A novel molecular simulation method for evaluating the endothermic transition of amylose recrystallite. Eur. Food Res. Technol. 229 (6), 853–858. https://doi.org/10.1007/s00217-009-1124-y.

Tu, Y., Huang, S., Chi, C., Lu, P., Chen, L., Li, L., Li, X., 2021. Digestibility and structure changes of rice starch following co-fermentation of yeast and Lactobacillus strains. Int. J. Biol. Macromol. 184, 530–537. https://doi.org/10.1016/j.ijbiomac.2021.06.069.

Villas-Boas, F., Facchinatto, W.M., Colnago, L.A., Volanti, D.P., Franco, C.M.L., 2020. Effect of amylolysis on the formation, the molecular, crystalline and thermal characteristics and the digestibility of retrograded starches. Int. J. Biol. Macromol. 163, 1333–1343. https://doi.org/10.1016/j.ijbiomac.2020.07.181.

Wani, A.A., Singh, P., Shah, M.A., Schweiggert-Weisz, U., Gul, K., Wani, I.A., 2012. Rice starch diversity: effects on structural, morphological, thermal, and physicochemical properties—a review. Compr. Rev. Food Sci. Food Saf. 11 (5), 417–436. https://doi.org/10.1111/j.1541-4337.2012.00193.x.

Ye, J., Hu, X., Luo, S., McClements, D.J., Liang, L., Liu, C., 2018. Effect of endogenous proteins and lipids on starch digestibility in rice flour. Food Res. Int. 106, 404–409. https://doi.org/10.1016/j.foodres.2018.01.008.

Zhu, B., Zhan, J., Chen, L., Tian, Y., 2020. Amylose crystal seeds: preparation and their effect on starch retrogradation. Food Hydrocolloids 105, 105805. https://doi.org/10.1016/j.foodhyd.2020.105805.

Zhu, F., 2017. Encapsulation and delivery of food ingredients using starch based systems. Food Chem. 229, 542–552. https://doi.org/10.1016/j.foodchem.2017.02.101.

Zhu, Y., Cui, B., Yuan, C., Lu, L., Li, J., 2022. A new separation approach of amylose fraction from gelatinized high amylose corn starch. Food Hydrocolloids 131, 107759. https://doi.org/10.1016/j.foodhyd.2022.107759.